

Mott and Band Insulator Transitions in the Binary Alloy Hubbard Model

N. Paris, A. Baldwin, and R.T. Scalettar

Physics Department, University of California, Davis, California 95616, USA

We use determinant Quantum Monte Carlo simulations and exact diagonalization to explore insulating behavior in the Hubbard model with a bimodal distribution of randomly positioned local site energies. From the temperature dependence of the compressibility and conductivity, we show that gapped, incompressible Mott insulating phases exist away from half filling when the variance of the local site energies is sufficiently large. The compressible regions around this Mott phase are metallic only if the density of sites with the corresponding energy exceeds the percolation threshold, but are Anderson insulators otherwise.

PACS numbers: 71.10.Fd, 71.30.+h, 75.10.Nr, 02.70.Uu

Introduction

The translationally invariant Hubbard model has long been studied as a model of itinerant magnetism and (Mott) insulating behavior. More recently, the possibility of unconventional (d -wave) superconductivity and spontaneously occurring charge inhomogeneities (stripes and checkerboards) has been explored, especially in the context of high temperature superconductivity.¹ Including disorder in the Hubbard Hamiltonian, for example in the form of a distribution of bond or site energies, imposes charge inhomogeneity externally and allows for the exploration of a number of other interesting phenomena such as the formation of Anderson insulating phases, possible transitions to metallic behavior driven by interactions^{2,3}, and the influence of disorder on magnetic correlations⁴.

A particularly interesting suggestion made recently^{5,6} concerns the possibility of Mott insulating phases away from half-filling in a Hubbard model corresponding to a binary alloy, that is, for which the probability distribution of site energies is bimodal, $P(\epsilon_i) = x\delta(\epsilon_i + \Delta/2) + (1-x)\delta(\epsilon_i - \Delta/2)$. The idea is that if Δ is sufficiently large compared to the bandwidth W , the non-interacting density of states will be split and an insulating gap will separate two density of states peaks of weight x and $1-x$. When an on-site repulsion U is turned on, these two peaks may in turn be Hubbard split by U . Thus in the limit $\Delta > U > W$ one can have Mott insulating phases at incommensurate densities $\rho = x$ and $\rho = 1+x$ which correspond to half-filling the two alloy subbands. A further interesting aspect of these Mott insulators is that they likely occur in the absence of antiferromagnetic ordering and its associated symmetry breaking, a phenomenon which complicates the metal-insulator transition in the translationally invariant Hubbard model at $\rho = 1$. Possible experimental realizations of the binary alloy Hubbard Hamiltonian in two dimensions include Co-Fe monolayers⁷. The nature of magnetism in such systems has been explored by first principles calculations⁸.

The previous studies of Mott transitions off half-filling within tight binding models were with dynamical mean field theory (DMFT). In this letter we will re-examine the physics of the binary alloy Hubbard model using de-

terminant Quantum Monte Carlo (DQMC) simulations and exact diagonalization. While these methods are restricted to finite size lattices, they allow us to examine some of the aspects of the effects of randomness like Anderson localization which are not accessible with DMFT.

The specific Hamiltonian we study is:

$$\hat{H} = -t \sum_{\langle lj \rangle \sigma} (c_{j\sigma}^\dagger c_{l\sigma} + c_{l\sigma}^\dagger c_{j\sigma}) + U \sum_l n_{l\uparrow} n_{l\downarrow} + \sum_l (\epsilon_l - \mu)(n_{l\uparrow} + n_{l\downarrow}) .$$

Here $c_{l\sigma}^\dagger$ ($c_{l\sigma}$) are the usual fermion creation (destruction) operators for spin σ on site l , $n_{l\sigma} = c_{l\sigma}^\dagger c_{l\sigma}$ is the number operator, and $\langle lj \rangle$ refers to near neighbor pairs on a two dimensional square lattice. t , μ and U are the electron hopping, chemical potential, and on-site interaction strength, respectively, and ϵ_l is a local site energy given by the bimodal distribution described previously. The bandwidth is $W = 8t$ when $\Delta = U = 0$.

This paper is organized as follows: We will first describe some of the details of our computational methodology. We then show results for the density as a function of chemical potential which illustrate the appearance of Mott plateaus off half filling, and also demonstrate the consistency of DQMC and direct diagonalization. Results for the participation ratio in the non-interacting limit suggest that the Mott plateaus at $\rho = x$ and $\rho = 1+x$ could in fact be rather different, a conclusion which we then confirm by calculating the temperature dependence of the conductivity. Finally, we examine the critical hopping t_c required to destroy the Mott plateau. We conclude by constructing the corresponding phase diagram.

Computational Methods

We study the alloy Hubbard Hamiltonian with exact diagonalization and DQMC⁹. The former approach is a standard application of the Lanczos algorithm to determine exactly the ground state wave function. We use $N = 8$ site lattices. In this case N is sufficiently small

that we can sum over all disorder realizations. In order to reduce finite size effects, we employ the boundary condition averaging method¹⁰. In the noninteracting limit, averaging over different hopping phases at the boundary for a finite lattice reproduces the thermodynamic limit spectrum exactly. For U nonzero, the finite size effects, while not eliminated, are dramatically reduced. Specifically, we implement a 2×4 cluster with two boundary phases (ϕ_x and ϕ_y), one boundary phase for each of the two independent, orthogonal boundaries. An average over the phase space area encompassed by $\phi_x = \{0, 2\pi\}$ and $\phi_y = \{0, 2\pi\}$ was done by selecting 10 to 100 (ϕ_x, ϕ_y) pairs.

In the DQMC approach, the partition function Z is expressed as a path integral by discretizing the inverse temperature β . The on-site interaction is then replaced by a sum over a discrete Hubbard-Stratonovich field¹¹. The resulting quadratic form in the fermion operators can be integrated out analytically, leaving an expression for Z in terms of a sum over all values of the Hubbard-Stratonovich field with a summand (Boltzmann weight) which is the product of the determinants of two matrices (one for spin up and one for spin down). The sum is sampled stochastically using the Metropolis algorithm. We present results for 6×6 lattices. We average over 5 – 10 realizations of the local site energies.

Equal time operators such as the density and energy are measured by accumulating appropriate elements, and products of elements, of the inverse of the matrix whose determinant gives the Boltzmann weight. For the conductivity, σ_{dc} , we employ an approximate procedure¹³ which allows σ_{dc} to be computed from the wavevector \mathbf{q} - and imaginary time τ -dependent current-current correlation function $\Lambda_{xx}(\mathbf{q}, \tau)$ without the necessity of performing an analytic continuation¹²,

$$\sigma_{dc} = \frac{\beta^2}{\pi} \Lambda_{xx}(\mathbf{q} = 0, \tau = \beta/2).$$

Here $\beta = 1/T$, $\Lambda_{xx}(\mathbf{q}, \tau) = \langle j_x(\mathbf{q}, \tau) j_x(-\mathbf{q}, 0) \rangle$, and $j_x(\mathbf{q}, \tau)$ the \mathbf{q}, τ -dependent current in the x -direction, is the Fourier transform of,

$$j_x(\ell, \tau) = i \sum_{\sigma} t_{\ell+\hat{x}, \ell} e^{H\tau} (c_{\ell+\hat{x}, \sigma}^{\dagger} c_{\ell\sigma} - c_{\ell\sigma}^{\dagger} c_{\ell+\hat{x}, \sigma}) e^{-H\tau}.$$

This approach has been extensively tested for the superconducting-insulator transition in the attractive Hubbard model¹³, as well as for metal-insulator transitions in the repulsive model^{2,14}.

In order to get further insight into the physics of Anderson localization, we also diagonalize the noninteracting system on lattices as large as $N = 64 \times 64$. We characterize the properties of the noninteracting eigenfunctions $|\phi_n\rangle$ through the scaling of the participation ratio,

$$\mathcal{P}_n = \left(\sum_{i=1}^N \langle i | \phi_n \rangle^4 \right)^{-1}.$$

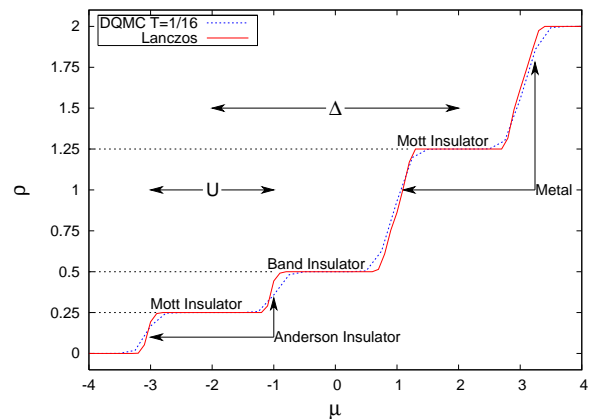


FIG. 1: (Color online) Density as a function of chemical potential for $W = 0.8$, $U = 2$, $\Delta = 4$ and $x = 0.25$. Solid line: ground state exact diagonalization of an eight site cluster; and dashed line: DQMC on 6×6 clusters with temperature $T = 1/16$. In the former case, results are averaged over all configurations with two sites with $\epsilon_A = -2$ and six sites with $\epsilon_B = +2$, and over different choices of the boundary phases. In the latter case, results are given for a single realization. The two methods give very similar results, with the DQMC somewhat rounded by finite temperature.

For an eigenfunction perfectly localized at a site i_0 , $\langle i | \phi_n \rangle = \delta_{i, i_0}$ we have, $\mathcal{P}_n = 1$, while for a perfectly delocalized eigenfunction $\langle i | \phi_n \rangle = 1/\sqrt{N}$, we have $\mathcal{P}_n = N$. In general, \mathcal{P}_n is a measure of the extent of the eigenfunction, that is, the number of sites for which $\langle i | \phi_n \rangle$ is non-negligible.

Results

We first demonstrate the existence of the Mott and band insulating phases by looking at the density as a function of chemical potential. Fig. 1 shows the case $U = 2$, $\Delta = 4$ and $x = 0.25$. We see a Mott insulating plateau extending from $\mu = (-\Delta - U)/2 = -3$ to $\mu = (-\Delta + U)/2 = -1$, in which the total density is $\rho = x = 0.25$. At $\mu = (-\Delta + U)/2 = -1$, the lower alloy subband becomes doubly occupied and $\rho = 2x = 0.5$. A second plateau then reflects the ‘band’ gap which must be surpassed to begin occupying the upper alloy subband, which is, like the lower subband, also Hubbard split.

In Fig. 1, the Mott plateaus revealed in $\rho(\mu)$ at $\rho = x = 0.25$ and $\rho = 1 + x = 1.25$ appear rather similar. We now argue that the nature of the states is, instead, quite different. For a square lattice in $d = 2$ the percolation threshold is $x_c = 0.5928$ ¹⁵. We therefore might expect that the non-interacting states with site energy $\epsilon_l = -\Delta/2 = -2$, out of which the $\rho = x$ plateau is built, are localized, since they constitute only a fraction $x = 0.25 < x_c$ of the sites in the lattice. Meanwhile, the non-interacting states with site energy $\epsilon_l = \Delta/2 = +2$, out of which the $\rho = 1 + x$ plateau is built, are delo-

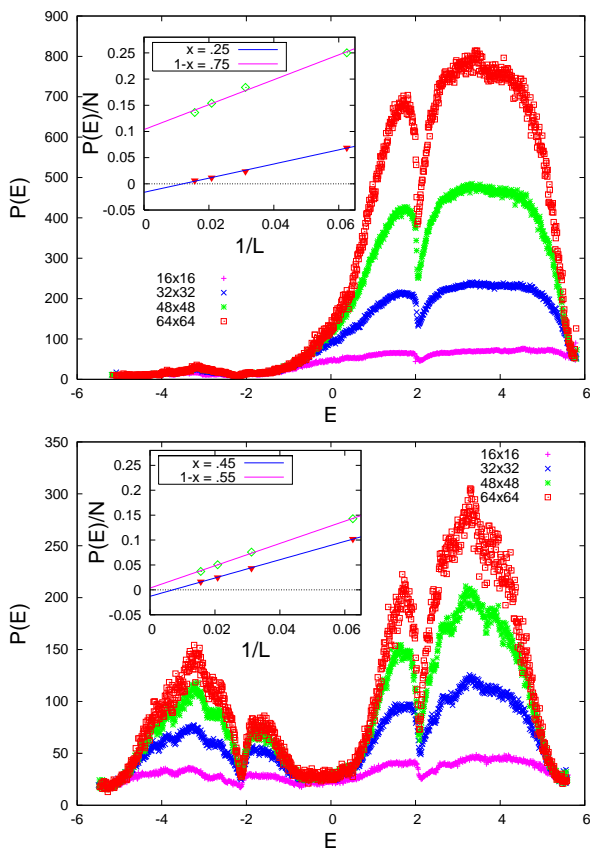


FIG. 2: (Color online) Upper panel: Participation ratio P as a function of the eigenenergy E for the alloy Hubbard Hamiltonian with $U = 0$, $\Delta = 4$, and $t = 1$. Results are shown for lattice sizes varying from $N = 16 \times 16$ to $N = 64 \times 64$. $P(E)$ is small for the lower alloy band which has only $x = 0.25 < x_c$ of the sites, but $P(E)$ in the upper alloy band has a significant fraction of N . The inset shows that $P(E)/N$ scales to a non-zero value as $N \rightarrow \infty$ for the upper band and zero for the lower band. Lower panel: The same for $x = 0.45$. Here both alloy subbands have a density below the percolation threshold, and both participation ratios scale to zero.

calized. This is illustrated in Fig. 2 where we show the participation ratio of the noninteracting system. States with energies corresponding to the upper alloy subband, which has a density exceeding the percolation threshold, extend over a macroscopic portion of the lattice. States in the lower alloy subband are localized.

We now use the temperature dependence of the conductivity to argue that the distinction between the two Mott insulating plateaus is preserved when the interaction U is turned on. Fig. 3 gives σ_{dc} as a function of μ for three different temperatures $T = 1/8$, $T = 1/12$ and $T = 1/16$. The conductivity is zero in both the Mott and band insulator phases. In the regions bracketing the upper alloy band, σ_{dc} is relatively large, and increases as T is lowered. That is, these regions are metallic. For densities bracketing the lower alloy subband, σ_{dc} is a factor of four smaller, and increases much less noticeably as T is lowered. Because of the sign problem, we are not able

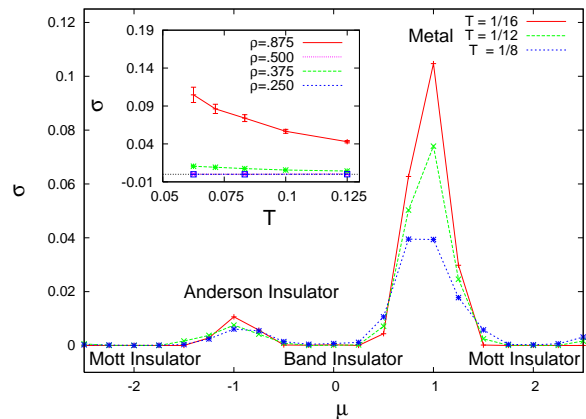


FIG. 3: (Color online) The conductivity σ_{dc} is shown as a function of chemical potential for several temperatures. Parameter values are as in Fig. 1. The upper alloy band, whose sites have a density larger than the percolation threshold, has a large σ_{dc} , which also increases as T is reduced (inset). The insulating phases have $\sigma_{dc} \approx 0$. The conductivity near the lower alloy subband is much smaller, and much more weakly temperature dependent than the upper.

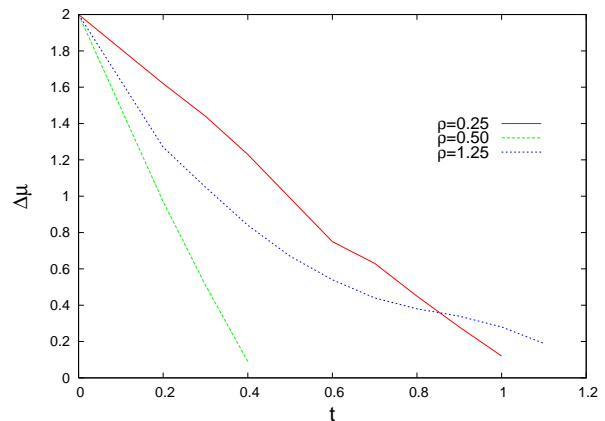


FIG. 4: (Color online) The length of the insulating plateaus $\Delta\mu$ is shown as a function of hopping t for $U = 2$, $\Delta = 4$ and $x = 0.25$, using exact diagonalization of $N = 8$ site clusters using boundary condition averaging. The Mott insulator plateaus at $\rho = x$ and $\rho = 1 + x$ are more robust than the band insulator plateau at $\rho = 2x$.

to obtain data for lower T . However, we believe that, as in the case of the Hubbard model with random site or bond energies^{2,14}, the conductivity will turn over and decrease as T is lowered further, reflecting the insulating character of the states.

We have presented DQMC results at $U = 2$, $\Delta = 4$ which correspond to on-site interaction and alloy site energy separation about twice and four times the bandwidth, respectively. The reason for these strong coupling values is that for larger t it is not possible to reach low enough temperatures to see clear plateaus in the density versus chemical potential plots. However, we argued

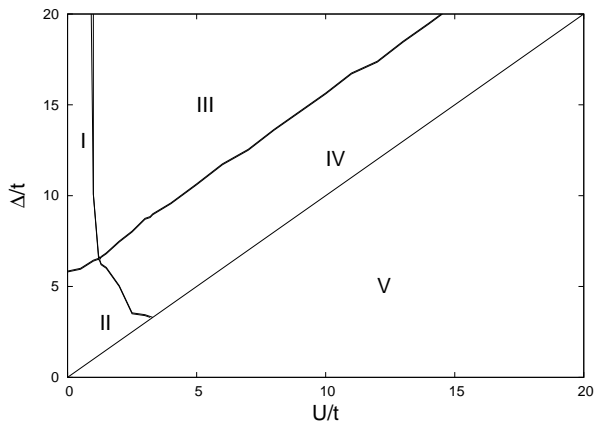


FIG. 5: Phase diagram of U/t vs. Δ/t . I: Band Insulator at $\rho = 0.50$ and no Mott Insulator. II: Metallic phase. III: Band Insulator at $\rho = 0.50$ and Mott Insulators at $\rho = 0.25$ and 1.25 . IV: Mott Insulator at $\rho = 0.25$ and 1.25 and no Band Insulator. V: $U > \Delta$, band insulator at $\rho = 0.25$ and 1.25 and Mott insulator at $\rho = 1.00$.

that diagonalization and DQMC gave consistent results (see Fig. 1), and we will now use the former approach to generate the ground state phase diagram at weaker couplings. As before, we average over different boundary condition phases to reduce finite size effects.

Fig. 4 shows the length of the three plateaus as the hopping t is increased for $U = 2$, $\Delta = 4$, and $x = 0.25$. The two Mott plateaus appear to vanish at roughly the same hopping strength, $t \approx 1$. The band insulator is less robust, and is destroyed when quantum fluctuations are only about half as strong. The reason is that when hopping off of one of the lower energy alloy sites for a Mott insulator you have to pay a cost of $\Delta = 4$. However, when you hop off of one of these sites for the band insulator you only have to pay the cost of $\Delta - U = 2$. This greater ease of such charge fluctuations for the band insulator makes its destruction by increasing t occur earlier.

Similar data for other choices of U and Δ allow us to generate the ground state phase diagram. In Fig. 5 we show four possible phases for the region of which $U < \Delta$. As in Fig. 4, large t that correspond to small U/t and Δ/t will suppress the insulating plateaus which results in a metallic phase. Taking the limiting case for small U/t and large Δ/t , we find one band insulating plateau

at $\rho = 2x$. Inversely, for small Δ/t and large U/t , we find two Mott phases at $\rho = x$ and $\rho = 1 + x$. For large U/t and Δ/t , both Band and Mott insulator phases coexist. The case for $U > \Delta$ will correspond to two band insulators at x and $1 + x$ and a Mott insulator at half-filling for sufficiently large values of U/t and Δ/t .

Conclusions

In this paper we have presented DQMC and diagonalization results for the phase diagram of the Hubbard model with binary alloy disorder. In agreement with previous treatments^{5,6}, we find Mott insulating behavior away from half-filling when the separation of the two site energies exceeds U . We extended the earlier results to characterize the nature of the compressible states above and below the Mott insulating plateaus by showing that their conductivity markedly differs. Together with the results for the participation ratio, our data suggest that for $x < x_c$ the lowest Mott plateau separates two compressible Anderson insulating regions, while the upper Mott plateau separates two compressible metallic phases.

Our results have focused primarily on $x = 0.25$, but different behavior would emerge for other values of x ¹⁶. For example, choosing a value of $x = 0.70 > x_c$ would not only produce Mott plateaus at $\rho = 0.70$ and 1.70 , but also create a lower Mott gap that are surrounded by metallic phases. Consequently, the upper Mott gap ($1 - x = 0.30 < x_c$) would be in between two Anderson insulating states.

A closer examination of magnetic correlations in this model is of interest, and will be the subject of future work. While we expect that disorder will suppress magnetism, as will the fact that the Mott phases are away from commensurate fillings, it is also the case that disorder can increase the exchange constant J and hence the Néel temperature in certain circumstances^{4,5,17}. Examining the real space magnetic correlations using DQMC would be a useful complement to previous DMFT studies.

We acknowledge support from the National Science Foundation under award NSF DMR 0312261, and useful input from M. Lovers.

¹ See, for example, E. Dagotto, Rev. Mod. Phys. **66**, 763 (1994), and references cited therein.

² P.J.H. Denteneer, R.T. Scalettar, and N. Trivedi, Phys. Rev. Lett. **83**, 4610 (1999).

³ M. Balzer and M. Potthoff, Physica B 359-361, 768 (2005).

⁴ M. Ulmke, V. Janiš, and D. Vollhardt, Phys. Rev. B **51**, 10411 (1995).

⁵ K. Byczuk, M. Ulmke, and D. Vollhardt, Phys. Rev. Lett. **90**, 196403 (2003).

⁶ K. Byczuk, W. Hofstetter, and D. Vollhardt, Phys. Rev. B **69**, 045112 (2004).

⁷ M. Pratzner and H.J. Elmers, Phys. Rev. Lett. **90**, 077201 (2003).

⁸ I. Turek, J. Kudrnovsky, V. Drchal, and P. Weinberger, Phys. Rev. B **49**, 3352 (1994).

⁹ R. Blankenbecler, D.J. Scalapino, and R.L. Sugar, Phys. Rev. D **24**, 2278 (1981).

¹⁰ J. Tinka Gammel, D.K. Campbell, and E.Y. Loh, Jr., Syn-

- thetic Metals **57**, 4437 (1993).
- ¹¹ J.E. Hirsch, Phys. Rev. B **31**, 4403 (1985).
- ¹² D.J. Scalapino, S.R. White, and S. Zhang, Phys. Rev. B **47**, 7995 (1993).
- ¹³ N. Trivedi, R.T. Scalettar, M. Randeria, Phys. Rev. B **54**, R3756 (1996).
- ¹⁴ P.J.H. Denteneer, R.T. Scalettar, and N. Trivedi, Phys. Rev. Lett. **87**, 146401 (2001).
- ¹⁵ D. Stauffer and A. Aharony, *Introduction to Percolation Theory* (Taylor and Francis, London 1992).
- ¹⁶ A. Alvermann and H. Fehske, Eur. Phys. J. B **48**, 295 (2005).
- ¹⁷ K. Byczuk and M. Ulmke, Eur. Phys. J. B **45**, 449 (2005).